APPLICATIONS OF INFRARED PHOTOACOUSTIC SPECTROSCOPY FOR WOOD SAMPLES[1]

Mon-lin Kuo

Assistant Professor
Department of Forestry
Iowa State University
Ames, IA 50011

John F. McClelland, Siquan Luo,[2]
Po-Liang Chien,[2] *R. D. Walker*[2]

Physicist, Visiting Scholar, Postdoctoral Fellow, Postdoctoral Fellow,
Ames Laboratory[3] U.S. Department of Energy
Ames, IA 50011

and

Chung-Yun Hse

Principal Wood Scientist
Southern Forest Experiment Station
Pineville, LA 71360

(Received February 1987)

ABSTRACT

Various infrared (IR) spectroscopic techniques for the analysis of wood samples are briefly discussed. Theories and instrumentation of the newly developed photoacoustic spectroscopic (PAS) technique for measuring absorbance spectra of solids are presented. Some important applications of the PAS technique in wood science research are discussed. The application of the Fourier transform infrared-photoacoustic spectroscopic (FTIR-PAS) technique is demonstrated by three preliminary studies of different forms of wood samples.

Keywords: Infrared spectroscopy, photoacoustic spectroscopy, wood sections, macerated wood elements, decayed wood samples.

INTRODUCTION

Infrared spectroscopy is an indispensable method for both qualitative and quantitative analysis of organic substances. Various infrared spectroscopic techniques have been used to study solid wood and the various constituents of wood (Liang et al. 1960; Harrington et al. 1964; Bolker and Somerville 1963; Sarkanen et al.

---

[1] Journal Paper No. J-12595 of the Iowa Agriculture and Home Economics Experiment Station (Project No. 2606), Ames, Iowa. This study was partly supported by Southern Forest Experiment Station, U.S. Forest Service, under cooperative agreement No. 19-83-040.

[2] Present addresses are: (S.L.) University of Science and Technology of China, Hefei, Anhui, PRC; (C.L.C.) Advance Fuel Research, 87 Church St., East Hartford, CT 06108; and (R.D.W.) Florida Dept. of Environmental Regulation, 26 Blair Stone Rd., Tallahassee, FL 32399.

[3] The Ames Laboratory is operated for the U.S. Department of Energy by Iowa State University under Contract No. W-7405-Eng-82. This research was supported partly by the Division of Chemical Sciences, Office of Energy Research and partly by the Assistant Secretary for Fossil Energy through the Pittsburgh Energy Technology Center.

Wood and Fiber Science, 20(1), 1988, pp. 132–145

1967) and to elucidate the mechanisms of delignification processes during pulping (Michell et al. 1965; Marton and Sparks 1967) and of aging processes of wood surfaces (Chow 1971; Feist and Hon 1984). Recently, because of increasing interest in the chemical pretreatment of wood to improve wood adhesion, infrared spectroscopy has been employed to investigate the mechanisms of chemical activation of wood surfaces and adhesive bond formation (Jenkin 1976; Rammon et al. 1982; Phillippou and Zavarin 1984).

The use of conventional infrared spectroscopic techniques for the analysis of solid samples presents some severe problems, including the opaqueness and light-scattering properties of samples and the low sample-to-noise signal available from dispersive instruments. With the advent of the commercial Fourier Transform Infrared (FTIR) instruments and different accessories, infrared spectra of solid samples can be obtained more rapidly with greater sensitivity. In this paper, various infrared spectroscopic techniques for the analysis of wood and wood component samples are briefly discussed, with the major emphasis being to introduce the newly developed Photoacoustic Spectroscopic (PAS) technique. The capability and potential of the FTIR-PAS technique for the analysis of wood samples is demonstrated by some exploratory experiments.

INFRARED SPECTROSCOPIC TECHNIQUES FOR WOOD SAMPLES

Transmission techniques

Light scattering and high optical density render the direct transmission spectroscopic analysis of wood samples very difficult. Light scattering can be greatly reduced by either impregnating thin wood sections with, or dispersing finely milled wood samples in, Nujol. Nujol, however, has interfering absorption bands at 2,850 to 3,000, 1,486, 1,379, and 720 cm^{-1}. Inorganic halides, when pressed into thin pellets, are an alternative that have a high transmittance throughout the midinfrared region. Therefore, transmission spectroscopic analysis of wood samples can be studied by embedding or dispersing them in halides such as KBr and KCl.

Liang et al. (1960) and Harrington et al. (1964) found that a thin wood section embedded in KBr gave a better IR spectrum than milled wood dispersed in a KBr pellet. The latter group of authors also found that pressing several thin wood sections in a KBr pellet gave a sharper spectrum than using a single wood section. There are situations, however, when wood sections are either difficult to obtain or relatively opaque such that wood samples must be studied in the form of fine powder dispersed in KBr pellets. Transmission spectroscopic analyses of isolated wood components, especially hemicelluloses and lignins, are generally studied by dispersing them in KBr pellets or Nujol.

With a careful control of sample concentration in KBr pellets and with a double beam spectrophotometer, it is possible to obtain difference spectra between sets of two different samples. For example, employing this technique, Bolker and Somerville (1963) were able to find differences between lignins in wood and pulp and isolated lignins.

Attenuated total reflectance (ATR) technique

An important method called attenuated total reflection (ATR) or internal reflection spectroscopy (IRS) for obtaining the infrared spectra of solids has been

described by Fahrenfort (1961). Initial ATR devices used a single-reflection prism and a variable angle of incidence to produce the desired spectra. Attenuated total reflection spectra can be markedly improved by using a multiple-reflection prism such as KSR-5. By placing a sample in very close contact with the reflecting surface of the prism, the energy that escapes temporarily from the prism is selectively absorbed by the sample. The spectrum of the internally reflected radiation is very similar to a typical transmission spectrum. The infrared band intensities are the equivalent of a shallow (approximately 5 μm or less) penetration into the sample and are completely independent of the sample thickness.

The ATR technique has been succesfully used to study undisturbed wood surfaces (Hse and Bryant 1966; O'Brian and Hartman 1969) and solid-phase changes of wood and wood components during chemical treatments (O'Brian and Hartman 1971; Jenkin 1976). Marton and Sparks (1967) also successfully used the ATR technique to determine the lignin content of unbleached kraft and sulfite pulps and uncoated paper samples.

In the ATR technique, the amount of infrared absorption is dependent on the area and efficiency of a close optical contact between the sample and the prism. Therefore, the intensity of absorption of a sample with an uneven and rough surface such as a wood section is a function of pressure applied to assemble the sample onto the prism. Thus, the pressure dependence of the ATR spectra is the main disadvantage of using the technique to study solid wood samples.

Diffuse reflectance technique

With the advent of the commercial Fourier transform spectrometers, diffuse reflectance spectroscopy has become an important method for qualitative and quantitative analysis of solid samples. In Diffuse Reflectance Infrared Fourier Transform Spectroscopy (DRIFT), a powdered sample is usually intimately mixed with an alkali halide powder such as KBr or KCl. When the powder matrix is irradiated, IR radiation is diffusely scattered in all directions. By a special optical arrangement, part of the diffuse radiation is refocused and directed to the detector. The ratio of the spectrum containing the sample to a KBr or KCl reference spectrum yields the diffuse reflectance spectrum of the sample, which is similar to the transmission spectrum of the sample measured in a KBr or KCl pellet. In some cases, diffuse reflectance spectra of neat samples can be measured.

Schultz et al. (1985a) found that the lignin, glucose, and xylose contents of wood determined by the DRIFT technique gave highly significant correlations with values obtained by conventional chemical analyses. Thus, the more rapid DRIFT technique can be used to analyze solid lignocellulosic materials with reasonable accuracy. The DRIFT technique has also been used to estimate degree of crystallinity of a variety of celluloses (Schultz et al. 1985b).

One of the major factors influencing diffuse relectance spectra is the particle size of the sample and the matrix material. Because the optical density is reduced with smaller sample particles, the sharpness and the relative intensity of absorption bands in a diffuse reflectance spectrum increase with decreasing particle size. Therefore, it is necessary to standardize particle size in any particular series of measurements (Krishnan 1984).

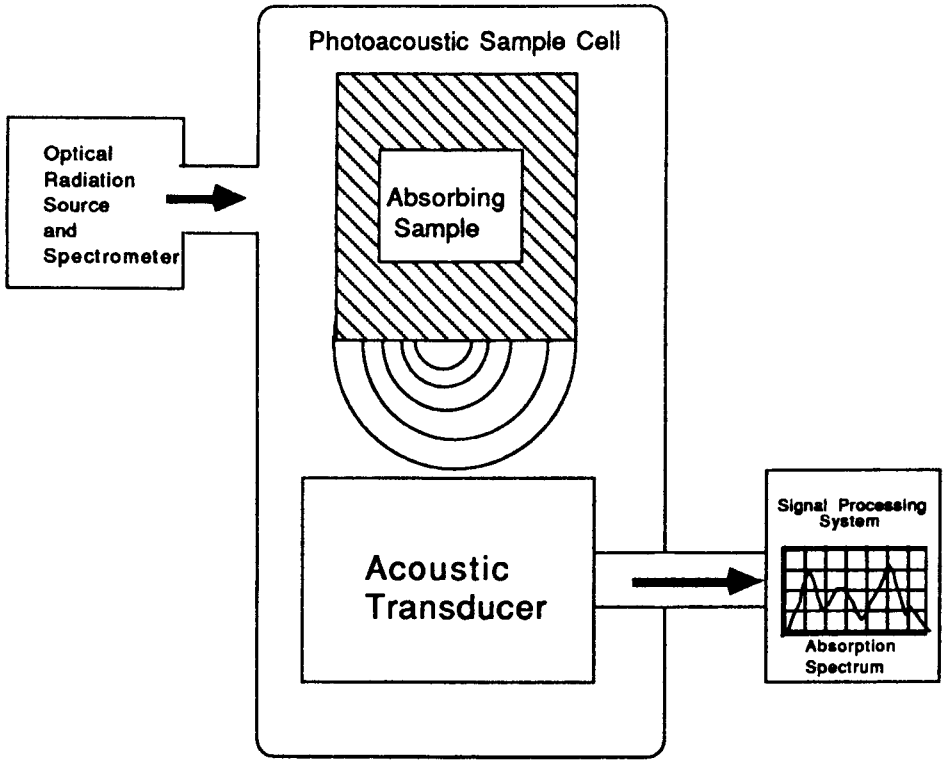

FIG. 1. Schematic of the photoacoustic spectroscopy technique (reproduced with permission from McClelland 1982).

PHOTOACOUSTIC SPECTROSCOPY OF SOLIDS

In photoacoustic spectroscopy (PAS) of solids, the sample is placed in an enclosed cell containing air or any other nonabsorbing gas and a sensitive microphone. The sample is then illuminated with a light beam that has an intensity modulation causing the intensity to oscillate in the acoustic frequency range. Nonradiative de-excitation processes convert part of or all the light absorbed by the solid into a heat oscillation within the sample with an amplitude proportional to the light absorption. The periodic flow of the converted heat into the surrounding gas produces pressure fluctuations in the cell that are detected by the microphone. Photoacoustic spectra can be obtained by recording the analog signal (which is proportional to the sample absorbance) from the microphone as a function of the wavelength of the incident light beam. A schematic of a typical photoacoustic measurement setup is shown in Fig. 1.

Basic theories of the photoacoustic effect and photoacoustic signal generation with solids have been given in detail by Rosencwaig (1975) and McClelland (1982). Figure 2 shows a schematic of the one-dimensional photoacoustic signal generation model. When the sample in a photoacoustic cell is illuminated with a light beam of power P_0, the sample's surface reflectivity, R, reduces the power just inside the surface of the sample to a value of $(1 - R)P_0$. Absorption of light during propagation in the sample further reduces the power in the light beam. At a sample

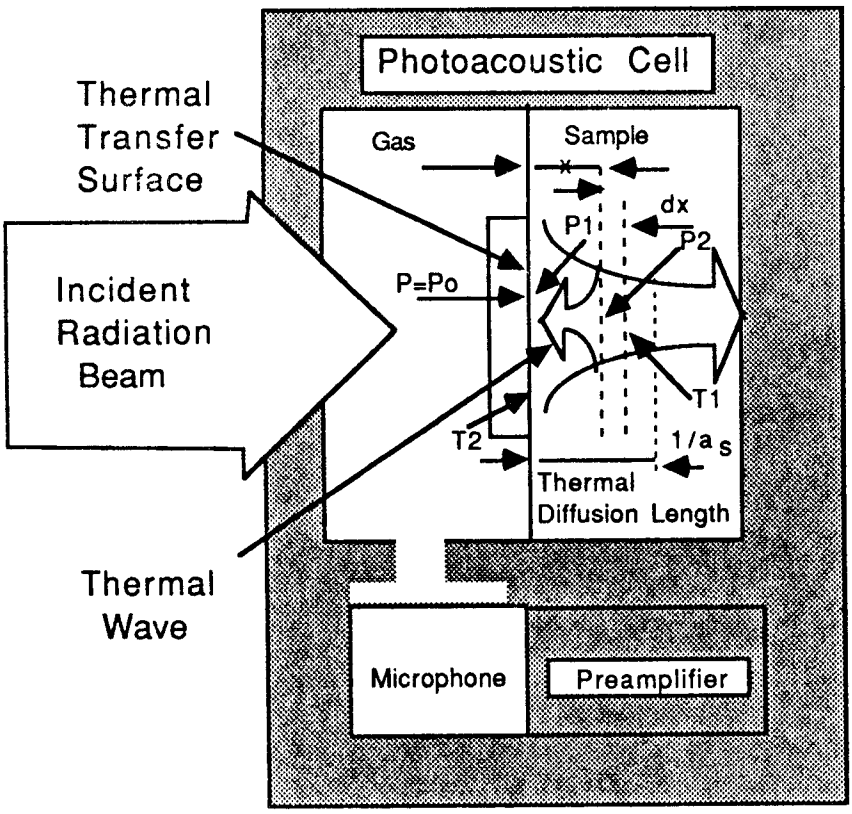

FIG. 2. Schematic of the one-dimensional photoacoustic signal generation model (reproduced with permission from McClelland 1982).

depth x_1 the power is reduced to $P_1 = (1 - R)P_oE^{-\alpha x_1}$, where α is the absorption coefficient. The absorption produces a temperature oscillation ΔT_1 in a layer Δx at depth x_1 with ΔT_1 proportional to $\alpha(1 - R)P_oE^{-\alpha x_1}\Delta x$. The layer of oscillating temperature generates thermal waves, which propagate toward both the irradiated and back sample surfaces. Thermal waves decay during propagation with a coefficient $a_s = (\pi f/\alpha T)^{1/2}$, where f is the light beam modulation frequency and αT is the sample's thermal diffusivity. The thermal waves transfer heat into the photoacoustic cell gas atmosphere at the irradiated surface, and gas pressure oscillations are generated. The pressure amplitude, ΔS_1, produced by the layer at x_1 is proportional to the temperature oscillation at the thermal transfer surface (irradiated surface) and is given by $\Delta S_1 = C\alpha(1 - R)P_oE^{-(\alpha+a_s)x_1}$, where C is a factor characteristic of the sample and cell.

The actual pressure signal, S, detected consists of contributions from all the sample layers to a depth permitted by the optical (α) and thermal (a_s) wave decay coefficients. S is found to vary linearly with increasing α but to gradually lose sensitivity at higher values of α, causing saturation (truncation) of strong absorbance bands. The loss of sensitivity occurs at lower values of α for higher α_t samples because the effective sample thickness that can be probed (estimated by $1/a_s$) is greater for these samples. Hence, just as in transmission spectroscopy, optically thick samples lead to saturation of strong absorbance bands.

TABLE 1. *Thermal ($1/a_s$) and optical ($1/\alpha$) wave decay lengths for a typical wood sample ($\alpha_t = 2 \times 10^{-3}$ cm²/sec).*

f (Hz)	$1/a_s$ (μm)	α (cm^{-1})	$1/\alpha$ (μm)
10	80	10	1,000
20	56	100	100
100	25	400	25
200	18	1,000	10
1,000	8	10,000	1
2,000	5.6		
10,000	2.5		

Because $1/a_s$ estimates the depth being thermally sensed in a FTIR-PAS measurement, there is the possibility of varying the measurement's thermal sensing depth by adjusting the light beam modulation frequency [$1/a_s = (\alpha_t/\pi f)^{1/2}$] and thereby of reducing saturation of strong bands or of obtaining spectral information for sample volumes extending different distances into the sample. In the latter case, however, the sample's optical and thermal properties as well as the modulation frequency range of the measurement dictate the actual depth range that can be investigated. These considerations are best understood by examining the situation for a specific measurement such as FTIR-PAS analysis of wood, which typically has a thermal diffusivity value of 2×10^{-3} cm²/sec. Table 1 summarizes the thermal and optical decay lengths for typical ranges of the light beam modulation frequency and the sample absorption coefficient, respectively.

In an FTIR measurement, the modulation frequency varies linearly along the wavenumber (υ) axis of spectra as given by f(Hz) = gυ(cm^{-1}). In this study, g = 0.05 cm/sec and the frequency started with 20 Hz at 400 cm^{-1} and increased linearly to 200 Hz at 4,000 cm^{-1}. Hence, the thermal sensing depth ($1/a_s$) range was 18 μm (4,000 cm^{-1}) to 56 μm (400 cm^{-1}) for samples with $\alpha_t = 2 \times 10^{-3}$ cm²/sec. The actual depth sensed cannot exceed $1/a_s$ at a given wavenumber or frequency, but it can be less if the sample's absorption length ($1/\alpha$) is less because thermal waves are not generated in layers that receive no light. Hence, the actual depth sensed at the peak of a hypothetical absorption band peak corresponding to a value α = 1,000 cm^{-1} is 10 μm regardless of where the band occurs in the mid-IR spectral range. On the other hand, if the peak corresponds to α = 400 cm^{-1}, an optical decay length of 25 μm results and the actual depth sensed is dictated by the optical absorption below f = 100 Hz or υ = 2,000 cm^{-1} and by the thermal sensing depth above υ = 2,000 cm^{-1}. So, for absorption band peaking at α = 400 cm^{-1}, the actual depth probed depends on where the band is located in the spectrum and will be 25 μm between υ = 400 and 2,000 cm^{-1} and decrease to 18 μm at υ = 4,000 cm^{-1}.

Generally, in practice, the actual depth probed is often difficult to specify in absolute terms because of uncertainties in the optical and thermal properties of samples and in details of signal-generation models applicable for a given sample geometry. Nevertheless the basic ideas just discussed are very useful for interpreting spectra. Measurements taken by using different modulation frequency ranges are highly useful when absorbance band saturation is suspected or when absorbance bands may vary with probe depth.

The instrumentation used in this study consisted of a Perkin-Elmer model 1800

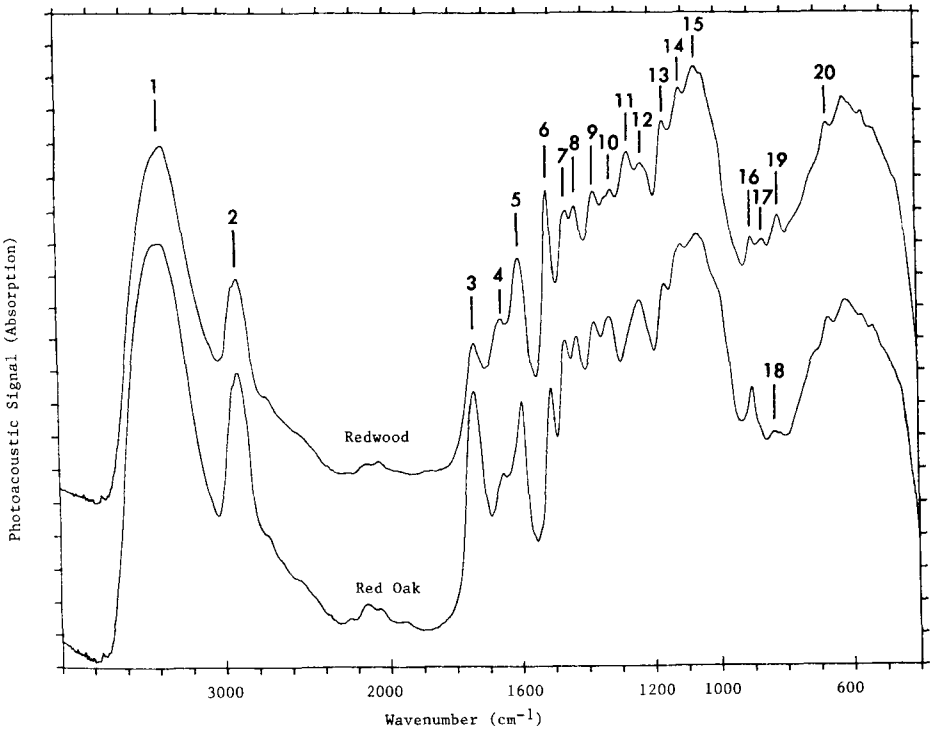

FIG. 3. Comparison of FTIR-PAS spectra of redwood and red oak radial sections (400 μm thick) taken from the microtomed surfaces.

FTIR spectrometer (Perkin-Elmer Corp., Main Ave., Norwalk, CT 06856, U.S.A.) and a MTEC Photoacoustics model 100 photoacoustic cell FTIR accessory (MTEC Photoacoustics, Inc., P.O. Box 1095, Ames, IA 50010, U.S.A.). FTIR-PAS spectra were obtained by adjusting sample spectra for a spectrum of carbon black to remove spectral variations not due to the sample. All spectra consist of 32 scan averages taken at 8 cm^{-1} resolution and plotted without any spectral smoothing. The sample chamber atmosphere was helium gas, selected for optimal signal generation efficiency. The gas was cryodried, and a desiccant was used in the sample chamber to reduce moisture band interferences. The FTIR mirror velocity was set at 0.05 cm/sec during this investigation, resulting in a modulation frequency range of 20 to 200 Hz.

EXPLORATORY STUDIES OF WOOD BY PHOTOACOUSTIC SPECTROSCOPY

Wood sections

To accommodate the photoacoustic cell used, circular samples 0.25 inch in diameter were prepared from wood sections by using a paper punch. Wood sections (400 μm thick) were obtained from dry samples with a microtome to minimize sample disturbance. For the 20 to 200 Hz modulation frequency range used, the thermal diffusion length of most wood samples is estimated to be between 18 and 56 μm, which is considered sufficient to indicate the bulk optical properties of the sample with the possible exception of narrow spectral regions having high peak absorbance.

TABLE 2. *Assignments of bands in the infrared spectrum of wood.*

Frequency		Assignment	References
1	3,300	Bonded O-H stretching	(5, 9, 12)
2	2,900	C-H stretching	(5, 9, 12)
3	1,730	C=O stretching in xylan	(5, 9, 12)
4	1,660	Keto-carbonyl conjugated with benzene ring	(1)
5	1,600	Benzene ring stretching in lignin	(1, 5, 9, 12)
6	1,505	Benzene ring stretching in lignin	(1, 5, 9, 12)
7	1,460	CH_3 deformation in lignin and CH_2 bending in xylan	(5, 9, 12)
8	1,425	CH_2 scissor vibration in cellulose	(9, 12)
9	1,370	CH_2 bending in cellulose and hemicellulose	(5, 9, 12)
10	1,325	CH_2 wagging vibration in cellulose	(9, 12)
11	1,275	Guaiacyl nuclei in lignin	(20)
12	1,230	Syringyl nuclei in lignin and C=O in xylan	(5, 20)
13	1,160	C-O-C asymmetric band in cellulose and hemicellulose	(5, 9, 12)
14	1,110	O-H association band in cellulose and hemicellulose	(5, 12)
15	1,050	C-O stretching in cellulose and hemicellulose	(5, 9, 12)
16	895	C1 group frequency in cellulose and hemicellulose	(5, 9, 12)
17	870	1,3,4-substituted benzene ring in softwood lignin	(5)
18	830	1,3,4,5-substituted benzene ring in hardwood lignin	(5)
19	810	1,3,4-substituted benzene ring in softwood lignin	(5)
20	680	COH out-of-plane bending in cellulose	(9)

FTIR-PAS spectra of a redwood and a red oak radial section are shown in Fig. 3 and assignments of various bands are given in Table 2. All known characteristic absorption bands of wood and differences between softwood and hardwood are clearly shown. A higher xylan content in red oak than in redwood is indicated by a stronger band at 1,730 cm^{-1} due to carboxyl and carbonyl groups in the xylan. A higher lignin content in redwood is indicated by a higher absorption intensity near 1,505 cm^{-1} than that in red oak. Spectral differences between redwood and red oak also are observed in the region between 1,300 and 1,200 cm^{-1}. Using model compounds, Sarkanen et al. (1967) found that the guaiacyl type (softwood lignin) absorbed near 1,275 and 1,230 cm^{-1} and that the syringyl type (the major type of hardwood lignin) absorbed only at 1,230 cm^{-1}. Although hardwood lignin also contains guaiacyl moieties, the absorption band at 1,275 cm^{-1} may have been obscured by a strong absorption at 1,230 cm^{-1} due to syringyl moieties of the lignin and to carbonyl groups of the xylan. Spectral difference due to the chemical nature of softwood and hardwood lignin is also observed in the region between 900 and 800 cm^{-1}. Harrington et al. (1964) attributed the absorption bands near 875 and 810 cm^{-1} in softwood to benzene ring substitution of the guaiacyl moieties and the band near 830 cm^{-1} in hardwood to syringyl moieties.

Figure 4 presents the result of an experiment comparing the FTIR-PAS spectra of a transverse and an oblique (45°) ponderosa section. The difference spectrum in Fig. 4 clearly shows that the absorption bands at 3,350 cm^{-1} and between 1,200 and 1,000 cm^{-1} in the oblique section are stronger than those in the transverse section. Because in the transverse section the cellulose chains are oriented perpendicular to the section normal, its band intensity at 3,350 cm^{-1} and between 1,200 and 1,000 cm^{-1} due to various functional groups in cellulose would be expected to be lower than those in the oblique and longitudinal sections (Liang et al. 1960). Therefore, spectral differences observed in Fig. 4 are due to differences

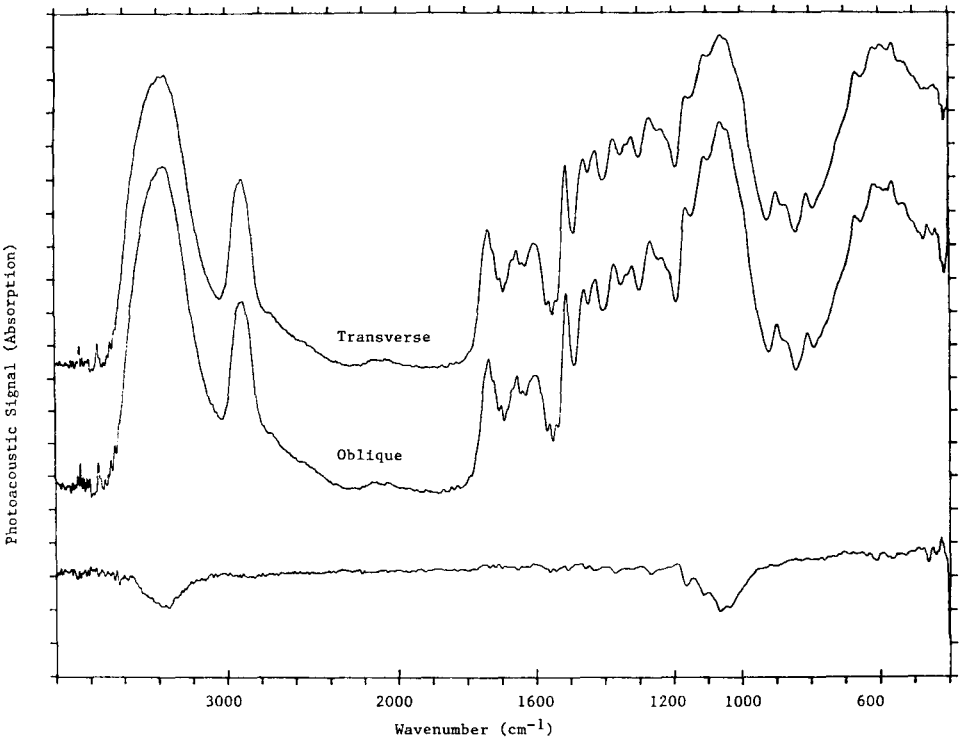

FIG. 4. Comparison of FTIR-PAS spectra of ponderosa pine transverse (top) and oblique (45° to the longitudinal direction, middle) sections. The lower spectrum is the difference between the transverse and oblique spectra.

in microfibrillar orientation relative to the section normal. Unfortunately, ponderosa pine does not have a xylan content high enough to detect the orientation of the xylan molecules. The absorption band at 1,730 cm^{-1} is considered stronger in ponderosa pine than that for common softwoods, which is most likely due to the carboxyl groups in resin acids in addition to carbonyl groups in the xylan.

An obvious advantage of the PAS technique over the KBr pellet method used by Liang et al. (1960) in studying the effects of microfibrillar orientation is that in PAS, the morphological characteristics of samples are not disturbed.

Decayed samples

Cottonwood samples with various degrees of decay (Table 3) caused by the brown-rot fungus *Gleoephyllum trabeum* were studied. Sample blocks 1 in × 1 in × 3/8 in (L) were ground with a Wiley mill, and wood meal passed through a 80-mesh screen was used for FTIR-PAS measurements. FTIR-PAS spectra of undecayed and decayed cottonwood samples are shown in Fig. 5.

A similar study of brown-rot decay of Buna wood (*Fagus crenata* Blume) was performed by Takahashi and Nishimoto (1967) using the KBr pellet technique. They found that the intensity of absorptions at 1,730, 1,380, and 895 cm^{-1} decreased progressively and that absorptions at 1,430 and 1,320 cm^{-1} increased slightly with increasing degree of decay. To more accurately analyze the FTIR-PAS spectra, a baseline method (Saad et al. 1980), where the baseline was con-

TABLE 3. *Analysis of the relative intensity of carbohydrate absorption bands in decayed samples using the lignin band at 1505 cm⁻¹ as the internal reference.*

Incubation duration (week)	Average weight loss (%)	Relative peak height				
		H1730/H1505	H1430/H1505	H1365/H1505	H1310/H1505	H895/H1505
Control	0	1.59	1.28	1.35	1.29	0.46
2	2.74	1.32	1.14	1.19	1.15	0.33
6	11.10	1.26	1.10	1.10	1.10	0.31
12	63.00	1.08	1.08	1.00	1.10	0.22

structed between 1,850 and 1,550 cm^{-1} and between 1,550 and 850 cm^{-1}, was used to calculate relative peak height of carbohydrate bands by using the lignin band at 1,505 cm^{-1} as the internal reference. Table 3 shows that the relative intensity of carbohydrate bands at 1,730, 1,425, 1,320, and 895 cm^{-1} all decreased with increasing degree of decay and that the absorption at 895 cm^{-1} was especially sensitive to detect incipient decay.

Figure 5 also shows other spectral changes associated with decay. Peak heights due to lignin at 1,595, 1,505, 1,460, and 835 cm^{-1} all increased as a result of decay. The lignin band at 1,275 cm^{-1}, which was not visible in the undecayed sample, developed into a shoulder of the band at 1,230 cm^{-1} in highly decayed samples. The appearance of the band at 1,275 cm^{-1} in decayed samples is mainly

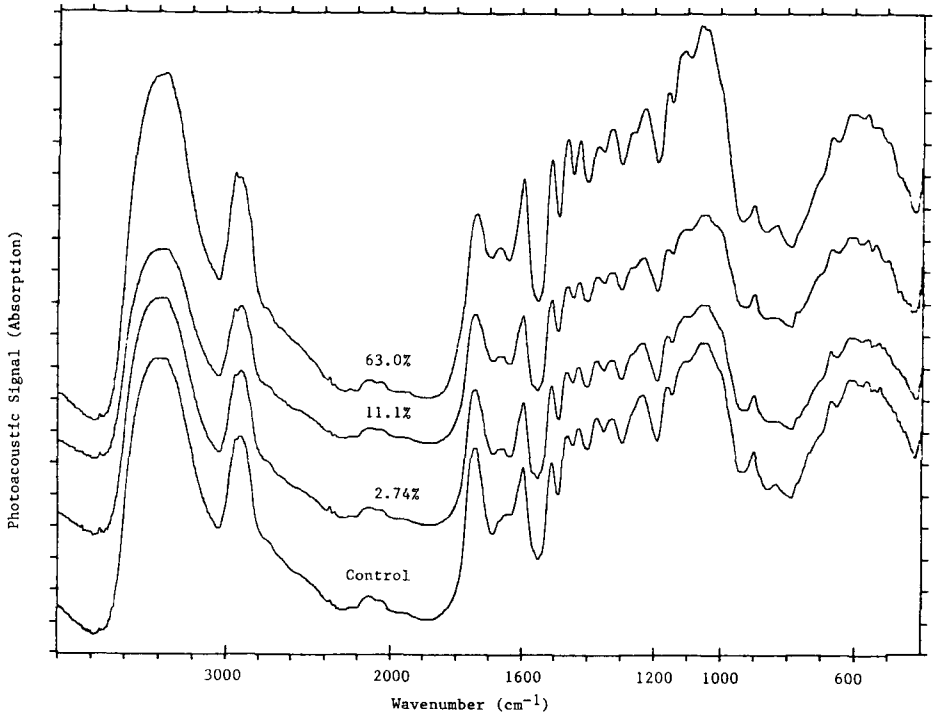

FIG. 5. FTIR-PAS spectra of eastern cottonwood samples with various degrees of decay by the brown-rot fungus *Gleoephyllum trabeum*. Numbers labelled on each spectrum represent average percentage weight loss of the sample due to decay.

due to the decrease of intensity at 1,230 cm^{-1} as a result of xylan degradation. The intensity near 1,660 cm^{-1} also increased as decay progressed. This band, which appears in spectra of wholewood and high-yield pulps but absent in most isolated lignins, has been assigned to α-keto groups conjugated with the benzene ring (Bolker and Somerville 1963).

Macerated wood elements

The FTIR-PAS technique is capable of obtaining good spectra from minute quantities of sample. A study was conducted to analyze cottonwood kraft (KAPPA No. 25) and groundwood (undelignified) fibers and vessel elements. A ring containing a fine-mesh stainless-steel screen of the type used in electron microscopy supported wood elements during photoacoustic measurements. Five fibers were used during each run to obtain each spectrum of kraft and groundwood fibers, whereas 15 vessel elements were used to obtain each spectrum of kraft and groundwood vessel elements.

FTIR-PAS spectra of kraft and groundwood fibers are shown in Fig. 6, and those of kraft and groundwood vessel elements are presented in Fig. 7. In the spectra of kraft wood elements, the characteristic lignin absorption bands at 1,505, 1,465, 1,275, 1,230, and 830 cm^{-1} were either greatly reduced or eliminated as a result of kraft pulping. The greatly reduced band at 1,730 cm^{-1} is evidently due to deacetylation of the xylan. Deacetylation of the xylan, together with lignin removal during pulping, also reduced the band at 1,230 cm^{-1}. The occurrence of a broad band near 1,600 cm^{-1} is mainly due to a band shifting from 1,730 cm^{-1} as a result of salt formation associated with carboxyl group (Mitchell et al. 1965).

Removal of lignin during pulping increased the intensity of the bands near 1,200, 1,170, 1,110, 1,050, 895, and 680 cm^{-1}, all of which have been assigned (Liang et al. 1960) to various characteristics of cellulose and other polysaccharides. Schultz et al. (1985b) found that the sharpness of cellulose IR peaks increases with increasing cellulose crystallinity. Therefore, increases in the intensity of this group of cellulose bands may be attributed to removal of lignin and most amorphous carbohydrates, which in turn, tends to increase crystallinity of residual cellulose. A comparison of the spectrum of groundwood vessel element with the spectrum of groundwood fiber reveals that the same group of cellulose bands absorbed more strongly in vessel elements than in fibers. It would be interesting to verify whether the degree of crystallinity of vessel cellulose is higher than that of fiber cellulose when the X-ray diffraction technique or other techniques are used.

Using an UV-EDXA technique, Saka and Goring (1985) found that the vessel wall had a higher lignin content than the fiber wall in white birch. The FTIR-PAS spectra of cottonwood groundwood fiber and vessel elements were used to estimate their relative lignin contents. A line constructed between 1,550 and 850 cm^{-1} was used as the baseline to calculate the relative peak height at 1,505 cm^{-1} by using bands at 1,430, 1,305, and 1,320 cm^{-1} as the internal references. Results shown in Table 4 indicate that the groundwood vessel elements had approximately 20% more lignin than groundwood fibers.

CONCLUSIONS

It has been demonstrated that high-quality infrared spectra of different forms of wood samples similar to optical spectra can be obtained by the FTIR-PAS

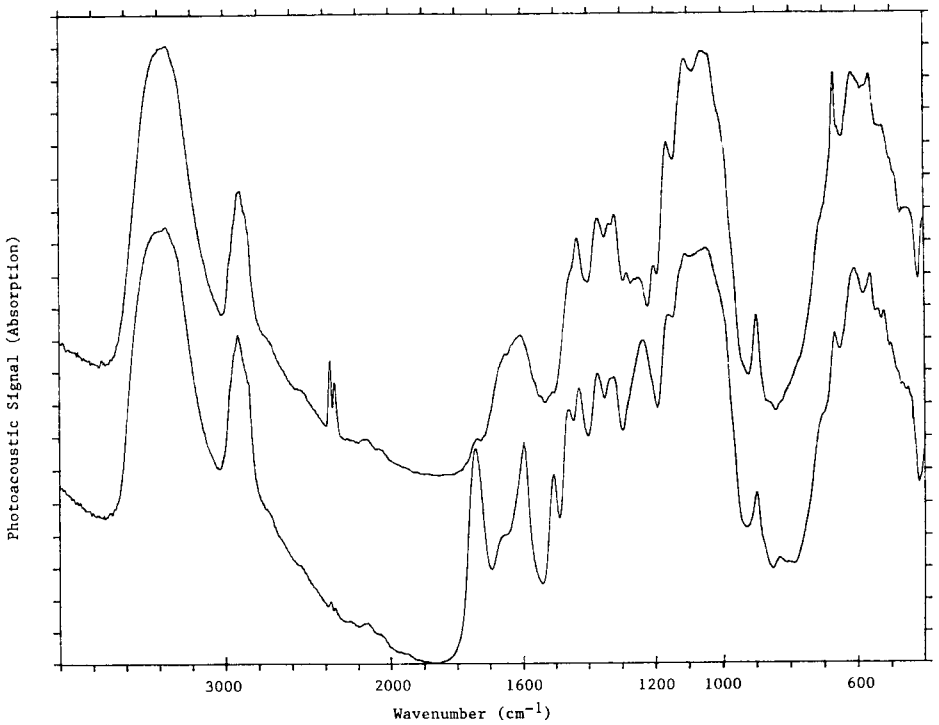

FIG. 6. FTIR-PAS spectra of eastern cottonwood kraft (KAPPA No. 25, top) and groundwood (bottom) fibers.

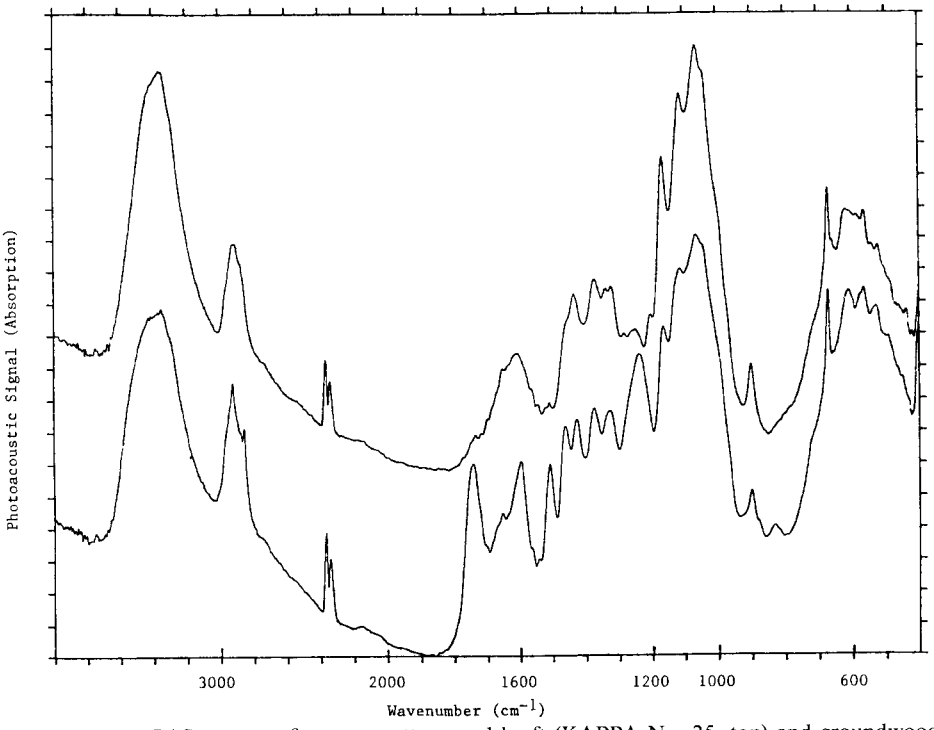

FIG. 7. FTIR-PAS spectra of eastern cottonwood kraft (KAPPA No. 25, top) and groundwood (bottom) vessel elements.

TABLE 4. *Relative lignin content of groundwood fibers and vessel elements estimated from relative peak height.*

Cell type		H1505/H1430	H1505/H1365	H1505/H1320
Vessel element	Relative peak height	0.70	0.66	0.67
Fiber	Relative peak height	0.56	0.53	0.54
Difference (%)		20	19.7	19.4

technique. In many instances, the photoacoustic method overcomes difficulties encountered in KBr pellet, diffuse reflectance, and attenuated total reflectance methods. Therefore, the FTIR-PAS technique has some important applications in wood science research. With its capability of variable depth sensing, the photoacoustic method could be useful to characterize wood surfaces and to study the mechanisms of wood surface activation and wood adhesive bond formation. Photoacoustic and diffuse reflectance spectroscopic studies of wood surfaces both in the infrared and ultraviolet-visible spectral ranges are planned.

REFERENCES

BOLKER, N. I., AND N. G. SOMERVILLE. 1963. Infrared spectroscopy of lignins. Part II. Lignins in unbleached pulps. Pulp Pap. Mag. Can. 64(4):T187–193.

CHOW, S. Z. 1971. Infrared spectral characteristics and surface inactivation of wood at high temperatures. Wood Sci. Technol. 5:27–39.

FAHRENFORT, J. 1961. Attenuated total reflection—A new principle for the production of useful infrared reflection spectra of organic compounds. Spectrochim. Acta 17:698.

FEIST, W. C., AND D. N. S. HON. 1984. Chemistry of weathering and protection. *In* R. M. Rowell, ed. The chemistry of solid wood. Advances in chemistry series 207. Am. Chem. Soc. Washington D.C.

HARRINGTON, K. J., H. G. HIGGINS, AND A. J. MICHELL. 1964. Infrared spectra of *Eucalyptus regnans* F. Muell. and *Pinus radiata* D. Dan. Holzforschung 18(4):108–113.

HSE, C. Y., AND B. S. BRYANT. 1966. The infrared analysis of the wood sections by attenuated total reflectance. J. Japan. Wood. Res. Soc. 12(4):187–191 (Engl.).

JENKIN, D. J. 1976. Infrared spectroscopy of chemically oxidized wood. Appl. Polymer Symp. 28: 1309–1320.

KRISHNAN, K. 1984. Different accessories, main applications and handling techniques. *In* T. Theophanides, ed. Fourier transform infrared spectroscopy, D. Reidel Publ. Co., Dardrecht/Boston/Lancaster.

LIANG, C. Y., K. H. BASSETT, E. A. MCGINNES, AND R. H. MARCHESSAULT. 1960. Infrared spectra of crystalline polysaccharides. VII. Thin wood sections. Tappi 43(12):1017–1024.

MARTON, J., AND H. E. SPARKS. 1967. Determination of lignin in pulp and paper by infrared multiple internal reflectance. Tappi 50(7):363–368.

MCCLELLAND, J. F. 1982. Photoacoustic spectroscopy. Anal. Chem. 55:89A.

MICHELL, A. J., A. J. WATSON, AND H. G. HIGGINS. 1965. An infrared spectroscopic study of delignification of *Eucalytus regnans*. Tappi 48(9):520–532.

O'BRIAN, R. N., AND K. HARTMAN. 1969. Infrared spectra of wood surfaces by attenuated total reflectance spectroscopy. Pulp Pap. Mag. Can. 70(4):T122–124.

———, AND ———. 1971. Air infrared spectroscopy study of the epoxy-cellulose interface. J. Polymer Sci. Part C, No. 34:293–301.

PHILLIPPOU, J. L., AND E. ZAVARIN. 1984. Differential scanning calorimetric and infrared spectroscopic studies of interactions between lignocellulosic materials, hydrogen peroxide, and furfuryl alcohol. Holzforschung 38(3):119–126.

RAMMON, R. M., S. S. KELLEY, R. A. YOUNG, AND R. H. GILLESPIE. 1982. Bond formation by wood surface reactions. Part II. Chemical mechanisms of nitric acid activation. J. Adhesion 14:257–282.

ROSENCWAIG, A. 1975. Photoacoustic spectroscopy of solids. Physics Today 28(9):23–29.

SAAD, S. M., R. M. ISSA, AND M. S. FAHMY. 1980. Infrared spectroscopic study of bagasse and unbleached high-yield soda bagasse pulps. Holzforschung 34:218–222.

SAKA, S., AND D. A. I. GORING. 1985. Localization of lignins in wood cell walls. *In* T. Higuchi, ed. Biosynthesis and biodegradation of wood components. Academic Press, Inc., NY.

SARKANEN, K. V., H. -M CHANG, AND B. ERICSSON. 1967. Species variation in lignins. I. Infrared spectra of guaiacyl and syringyl models. Tappi 50(11):572–575.

SCHULTZ, T. P., M. C. TEMPLETON, AND G. D. MCGINNIS. 1985a. Rapid determination of lignocellulose by diffuse reflectance Fourier transform infrared spectrometry. Anal. Chem. 57:2867–2869.

———, G. D. MCGINNIS, AND M. S. BERTRAN. 1985b. Estimation of cellulose crystallinity using Fourier Transform-Infrared spectroscopy and dynamic thermogravimetry. J. Wood Chem. Technol. 5(4):543–551.

TAKAHASHI, M., AND K. NISHIMOTO. 1967. Studies on the mechanism of wood decay (2). Changes in infrared spectra of Buna and Sugi wood. Wood Res. No. 42:1–12.